Journal of Solid State Chemistry 181 (2008) 1659–1669

Contents lists available at ScienceDirect

Journal of Solid State Chemistry

journal homepage: www.elsevier.com/locate/jssc

Ordered mesoporous silica-based inorganic nanocomposites

Qingqing Wang, Daniel F. Shantz *

Artie McFerrin Department of Chemical Engineering, Texas A&M University, Mail Stop 3122, College Station, TX 77843, USA

ARTICLE INFO

Article history:
Received 29 January 2008
Received in revised form
19 May 2008
Accepted 2 June 2008
Available online 12 June 2008

Keywords:
Ordered mesoporous silicas
Nanoparticles
Synthesis
Nanowires
Thin films

ABSTRACT

This article reviews the synthesis and characterization of nanoparticles and nanowires grown in ordered mesoporous silicas (OMS). Summarizing work performed over the last 4 years, this article highlights the material properties of the final nanocomposite in the context of the synthesis methodology employed. While certain metal-OMS systems (e.g. gold in MCM-41) have been extensively studied this article highlights that there is a rich set of chemistries that have yet to be explored. The article concludes with some thoughts on future developments and challenges in this area.

Published by Elsevier Inc.

1. Introduction

Developing the ability to control material properties such as composition, structure, and morphology at the nanometer scale will lead to both intellectual advances in material design as well as societal benefits through enabling of new technologies and improvements in existing ones. In the last 10 years the field of nanotechnology has witnessed an explosive growth. Take for example the synthesis of nanoparticles, nanowires, and other multidimensional nanostructures. Chemists now have the ability to synthesize materials with highly tailored compositions, chemical structures, and particle sizes. Thus nanoparticles are beginning to make contributions and inroads into fields as diverse as magnetic materials, biological sensing, and chemical warfare agent sensing/destruction.

Ordered mesoporous silicas (OMS) are another class of materials possessing unique properties at the nanoscale. since their initial discovery by the Mobil labs in the early 1990s [1,2] these materials have been heavily investigated [3–8]. These porous solids have desirable properties including highly uniform pore sizes in the 2–10 nm range that possess long-range order, despite that the matrix material is amorphous silica. Originally it was hoped that these materials would be large-pore versions of zeolites, i.e. possess comparable thermal stability and acidity [9]. This would enable, among other things, the cracking of large hydrocarbons too large to enter the pores of zeolites. While this has not come to pass, OMS phases show considerable promise as model supports for a variety of applications, as well as intriguing possibilities as nanocontainers, wherein chemistry can be performed to generate novel nanocomposites. The functionalization of OMS materials, particularly chemical grafting of homogeneous catalysts, and their use as catalyst supports is an active field of study and has been extensively reviewed elsewhere [9–13]. OMS have also been studied extensively for separations, drug release, and a variety of other potential applications. The use of OMS phases as containers for nanoparticle/nanowire growth is the focus of this Review/Perspectives article. That these materials possess uniform pores possessing long-range ordering, and that the pore surface contains silanol groups facilitating well-developed silane chemistry for tuning surface properties makes these materials in many ways model supports for assembling nanocomposite materials. Fig. 1 summarizes some of the basic properties of the most frequently studied OMS phases and the methods one can use to analyze them [13].

This contribution summarizes the generation of OMS-nanoparticle and -nanowire composites. While much of this work originates from the catalysis community, works are beginning to emerge where the inorganic phase occluded in the OMS pores has applications beyond catalysis (e.g. magnetic, optical materials). In this Review/Perspectives article, the literature since 2004 will be reviewed, focusing on the synthesis of metal nanoparticles and nanowires. Earlier works have been reviewed and summarized elsewhere [14–17]. The review will emphasize the various synthesis methodologies used to date, attempting to correlate and understand how the material synthesis method impacts the properties of the occluded phase. Also whether powders or films

* Corresponding author.
E-mail address: Shantz@chemail.tamu.edu (D.F. Shantz).

0022-4596/$ - see front matter Published by Elsevier Inc.
doi:10.1016/j.jssc.2008.06.015

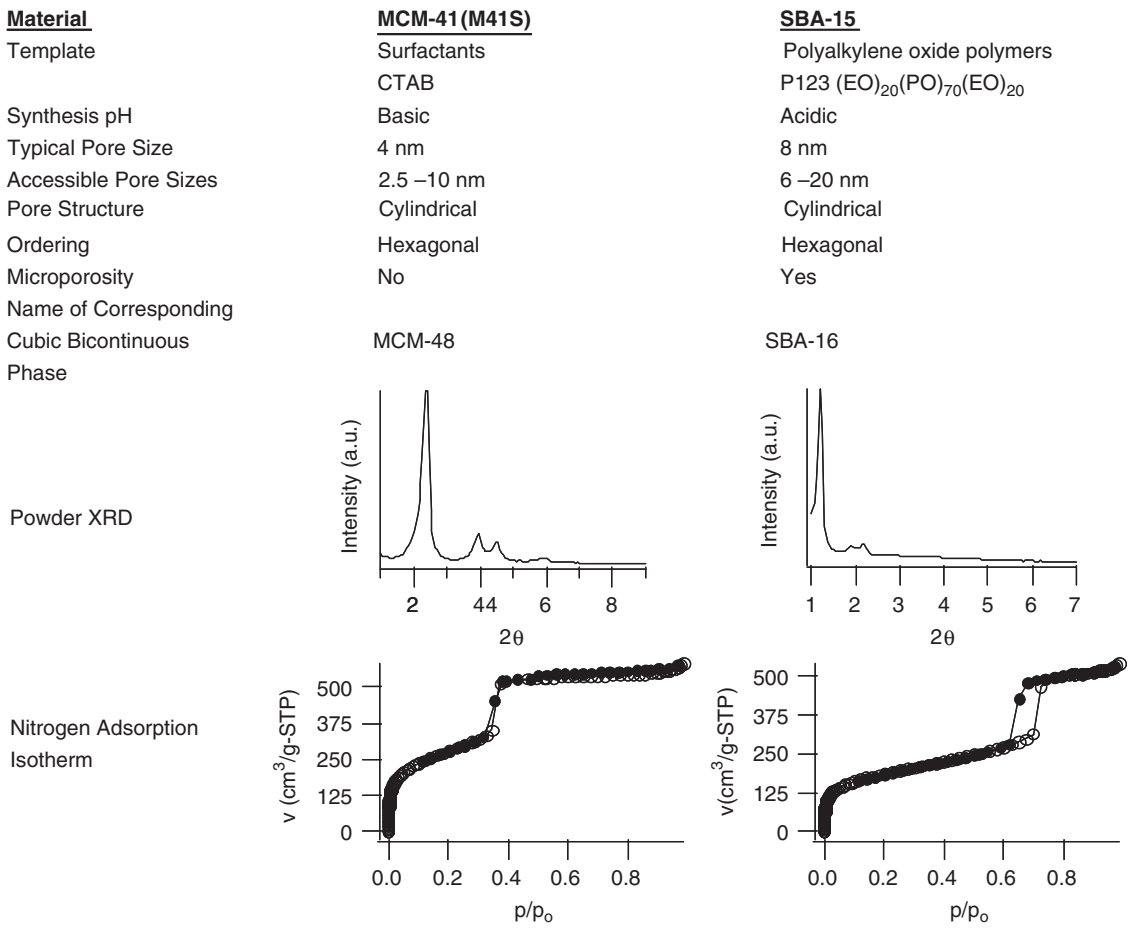

Fig. 1. Comparison of various properties of MCM-41 and SBA-15. Figure used from Ref. [13] with permission of the Institute of Physics.

of OMS materials were used as the substrate will be noted. OMS thin films are a potentially attractive matrix phase as they are more amenable for device fabrication and also present a straightforward means to orient the nanostructured material formed. The article will conclude with the authors' perspectives on the future of this area, some unresolved problems facing the field, and potential opportunities.

2. Metal nanoparticles in OMS phases

Most studies of OMS-nanoparticle composites have focused on forming metal nanoparticles in OMS, particularly of late transition metals such as silver, gold, platinum, and palladium. There are several driving forces for this including their relative ease of synthesis, the existing body of literature from the catalysis community of metal particles on other substrates and their catalytic relevance, particularly for platinum and palladium. Gold is a relatively late arrival in the catalysis community. However, gold colloids have been known for nearly 150 years from Faraday's work in the 1850s and were some of the early cluster phases investigated in solution [18]. An additional driving force for investigating gold particles on OMS came from Haruta's lab when in the early 1990s he showed that small gold particles were catalytically active for a variety of reactions, most notably low-temperature CO oxidation [19,20]. Each metal will be treated separately and the results organized by the synthesis methods used. Most investigations fall into one of three categories: deposition/precipitation on the OMS support (also often referred to as incipient wetness impregnation), direct synthesis wherein the nanoparticle reactants are added to the OMS synthesis mixture, or impregnation of preformed nanocrystals.

2.1. Gold

2.1.1. Post-synthetic deposition and other reagent impregnation methods

Abhaya Datye and coworkers at the University of New Mexico, along with collaborators in other labs, have published a series of papers investigating the formation of gold nanoparticles in a variety of OMS supports. This work has been very recently reviewed elsewhere [21], so only a few key observations will be made here. The methodology employed was to synthesize the OMS phase, remove the surfactant via calcination, graft aminosilanes to the OMS surface, and then impregnate the amine-functionalized OMS with hydrogen tetrachloroaurate hydrate solution, pH adjusted to 7 with 1 M NaOH. The target loading of Au was 5 wt%. The samples were then washed with water, dried under vacuum and reduced in flowing hydrogen at 200 °C. The authors showed that OMS formed via aerosol formation possessing coiled or wormhole-like pores resulted in increased gold nanoparticle stability as compared to conventional MCM-41 with straight pores [22]. This conclusion was based on both catalytic testing of the materials for low-temperature CO oxidation and also HAADF TEM which indicated the particles were larger in MCM-41

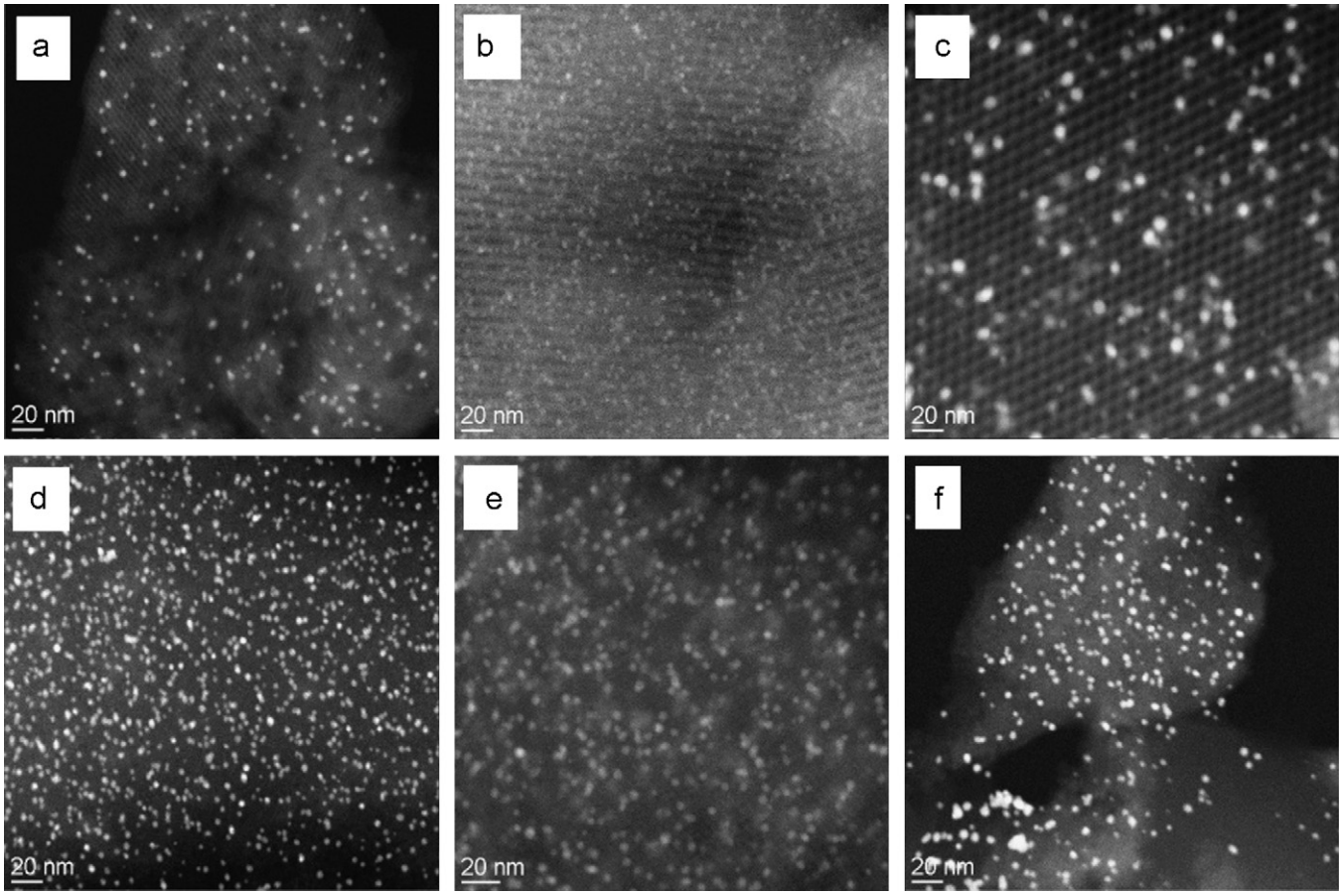

Fig. 2. SEM imgaes of Au/SBA-12 materials: (a) SE image at 2 kV, (b) BSE images at 2 kV, (c) SE images at 5 KV, and (d) BSE images at 5 kV. The Au particles appear to be on the external surface as there is no change in the number of particles observed with changes in the accelerating voltage. Figure used from Ref. [23] with permission of the American Chemical Society.

as compared to the aerosil phase. Subsequent work [23] investigated the role of the OMS substrate on the composite properties as several OMS phases including MCM-41, SBA-15, SBA-11, SBA-12, and HMM-2 were investigated. HAADF STEM, TEM, SEM, and BSE were used to analyze these samples. The authors observed some structure sensitivity in that for a phase such as SBA-12 and SBA-11 significant amounts of Au particles were formed on the outer surface whereas this was not the case with MCM-41. Fig. 2 shows an example of the SEM work performed. The authors also investigated the occlusion of heteroatoms ($M=$ Co, Fe, and Al at a Si/$M=30$) in the OMS framework to observe what effect this had on Au nanoparticle stability [24]. The main conclusion was that the inclusion of cobalt improved the catalytic activity of the materials. Again numerous EM methods were used to analyze the samples.

Work from Chao's lab was based on a similar synthetic approach. However, instead of amines Chao's lab grafted trimethoxypropyltrimethylammonium chloride silane ($(CH_3O)_3Si(CH_2)_3NH_3^+Cl^-$ [25,26]. The authors used electrostatic interactions to complex the gold precursor (usually $HAuCl_4$) to SBA-15 followed by reduction. In one report the authors looked at the effect of pH during gold complexation [25] as well as the effect of complete rinsing of the materials before gold reduction. Using primarily X-ray absorption spectroscopy (XAS) the authors showed that the pH of complexation affects the particle size (higher pH, smaller particles) and at pH 8 the chlorine was effectively displaced. In another work this group [26] studied the effect of ethanol versus aqueous solutions for the gold impregnation step. Using a variety of methods including UV–Vis spectroscopy, electron microscopy and XAS the authors characterized both small (<10 nm) and larger (>10 nm) particles. The former were associated with the pore interior, the latter with the particle external surface.

Nakamura et al. [27] have reported Au-OMS materials based on a modification of their previously published reports for synthesizing highly uniform mesoporous silica nanospheres [28]. Here they report the synthesis of thiol-functionalized OMS spheres, which were then treated with $HAuCl_4$ in a mildly acidic solution. Through multiple washings with dilute HCl the authors report nearly all gold complexes on the exterior surface were removed. Using a variety of methods including Raman spectroscopy, UV–Vis, and electron microscopy the authors verified the formation of small Au particles (Fig. 3). These were some of the most thoroughly characterized Au-OMS nanocomposites reported.

In addition to using organic ligands to complex gold other works have reported taking pure silica OMS materials and depositing a thin layer of titanium using sol–gel methods. This was likely inspired by the catalysis work from Haruta's lab that demonstrated TiO_2 supports facilitate high gold dispersion. These materials are then impregnated with gold precursors. Bandyopadhyay et al. [29], using MCM-48 as a support phase employed post-synthetic impregnation of tetrabutylorthotitanate in acetone to achieve a material containing approximately 15 wt% titania. This material was then impregnated with $HAuCl_4 \cdot 3H_2O$ and the pH adjusted to pH 7. Three cycles of such a treatment resulted in a material with a gold loading of approximately 3 wt%. The materials were characterized using numerous methods including X-ray diffraction, TEM, and XAS as well as catalytic testing. Fig. 4

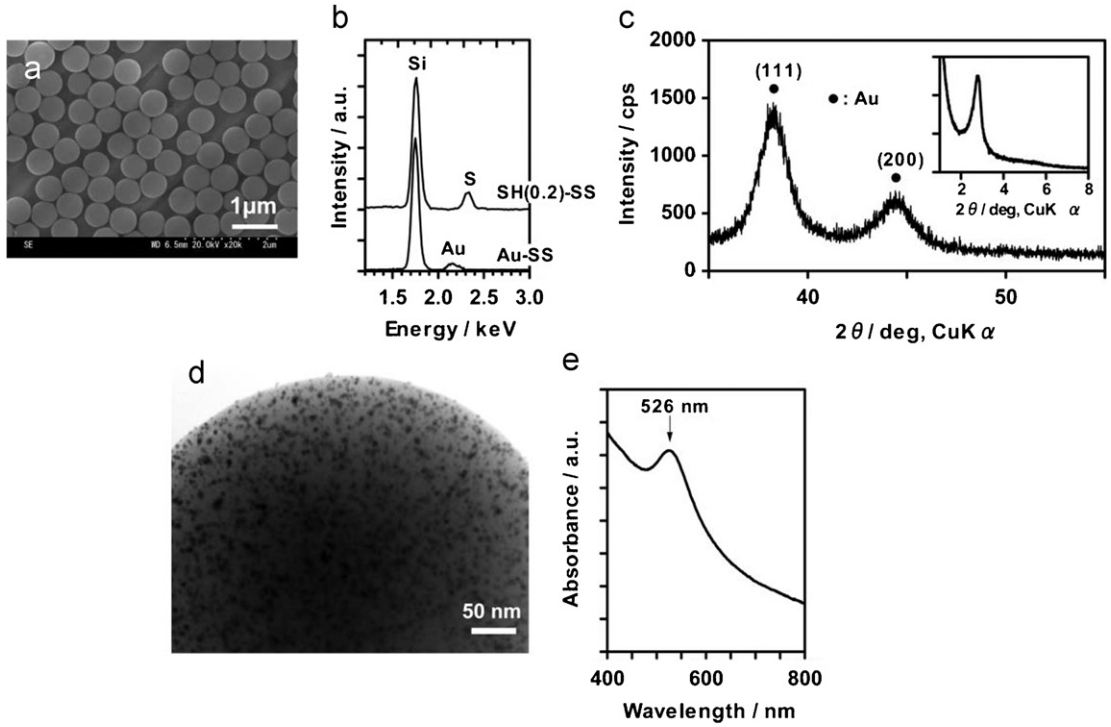

Fig. 3. (a) SEM images of Au/thiol-functionalized OMS nanospheres. (b) EDX spectra of thiol-functionalized OMS nanospheres (upper) and Au/thiol-functionalized OMS nanospheres (lower). (c) XRD pattern for thiol-functionalized OMS nanospheres (inset: small-angle XRD pattern). (d) TEM image of Au/thiol-functionalized OMS nanospheres. (e) Adsorption spectrum for Au/thiol-functionalized OMS nanospheres dispersed in toluene. Figure used from Ref. [27] with permission from the Royal Society of Chemistry.

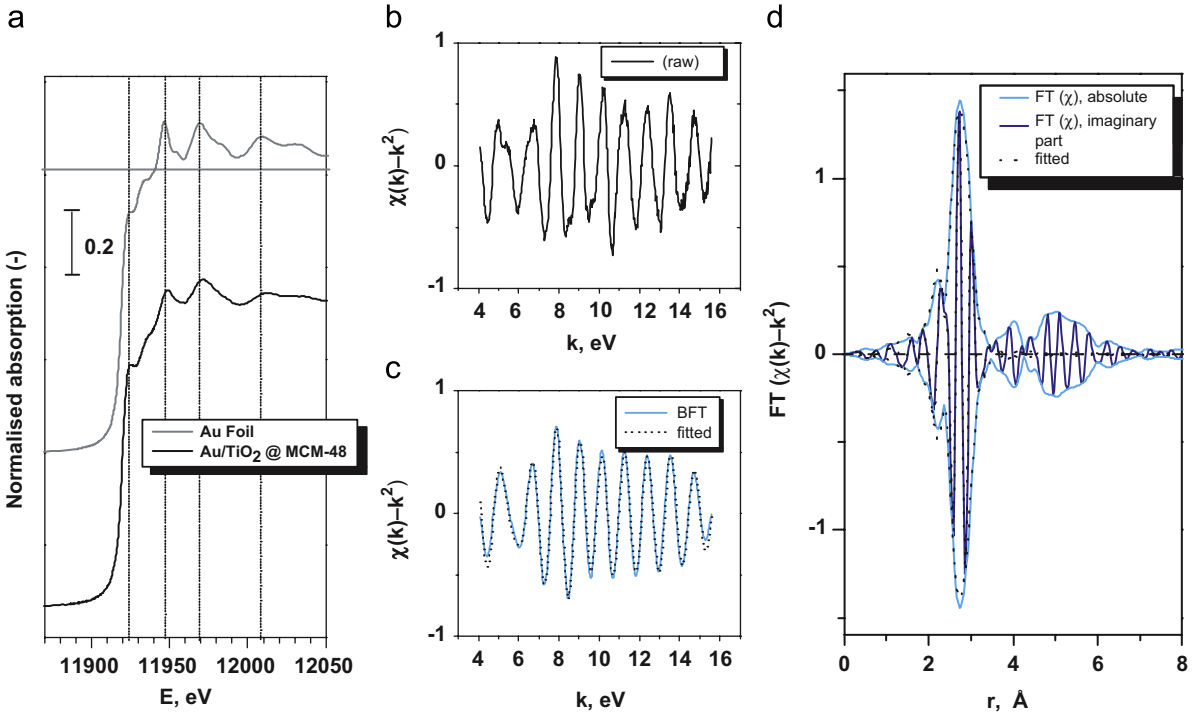

Fig. 4. k^2-weighted Au L_{III}-edge absorption spectra of Au/TiO_2-MCM-48, showing (a) the XANES compared to gold foil, (b) the measured $\chi(k)$, (c) the model $\chi(k)$ and (d) the Fourier transform and model Fourier transform. Figure used from Ref. [29] with permission from Elsevier.

shows the X-ray spectroscopy results. The two main conclusions from the work were that the absence of light was essential to the gold nanoparticle activity in CO oxidation, and that the particles appeared resistant to sintering at elevated temperatures, consistent with their inclusion in the MCM-48 mesopores. Yan et al. [30] reported a somewhat similar approach forming layers of TiO_2 on SBA-15. Their gold impregnation approach is somewhat different in that the pH was slightly higher than several reports (i.e. above 7). Relying primarily on TEM the authors claimed to have formed very small, 0.8–1.0 nm, Au particles in SBA-15.

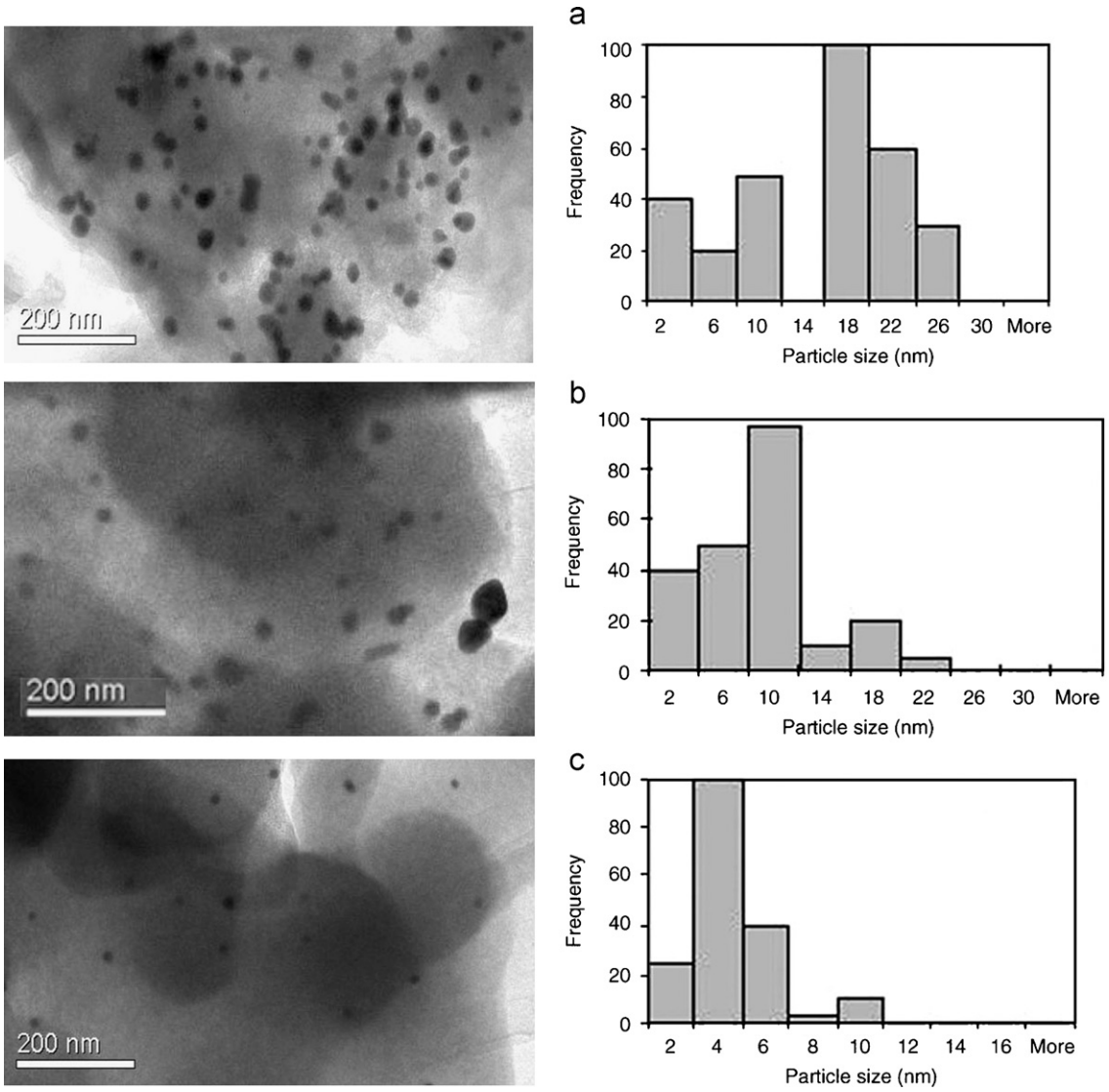

Fig. 5. TEM images of Au/MCM-48 obtained using supercritical CO_2 pressures of (a) 7 MPa, (b) 10 MPa, and (c) 12 MPa. Figure used from Ref. [33] with permission of Wiley VCH.

Studies have also reported the synthesis of Au nanoparticles without any special surface modification of the OMS phase. Kan et al. [31] used a classic impregnation/reduction approach to make gold particles on OMS monoliths. Using primarily optical spectroscopy and TEM the authors showed that formation of nanowires or spherical nanoparticles depended on the annealing conditions. High-temperature annealing favored spherical particles whereas low-temperature annealing favored wires. In this work many of the particles appeared to be on the outer surface of the material based on TEM/SEM. Tsung et al. [32] investigated gold particle/wire formation in OMS fibers using a simple impregnation/reduction scheme. Using X-ray diffraction, UV–Vis spectroscopy, and TEM the authors showed that the preparation method, particularly the degree of sample dehydration prior to reduction and reduction conditions, can be used to manipulate whether spherical particles or ellipsoids were formed. Their conclusions were generally in line with Kan and coworkers. It was also noteworthy that the authors showed that the major axes of the ellipsoids could be oriented in different directions with respect to the fiber axis by manipulating the OMS fiber nanostructure. Chatterjee et al. [33] have shown a fairly unique approach using MCM-48 as a substrate that resulted in the ability to easily control the size of the Au nanoparticles formed. In their work the $HAuCl_4$ and OMS mixture were heated to 70 °C and pressurized with 2 MPa of hydrogen, at which point CO_2 was injected at pressures between 7 and 12 MPa. The most interesting result, shown in Fig. 5, was the clear inverse relation between particle size and CO_2 pressure. It seemed likely that the particles formed at lower pressures were on the external surface of the MCM-48 given they are much larger than the pore size.

2.1.2. Direct synthesis methods

Several labs have also employed direct synthesis methods, wherein the gold precursor is added directly to the synthesis mixture. Akolekar and Bhargava [34] added the gold salt (not identified) directly to the MCM-41 synthesis mixtures; the materials had target Si/Au ratios of 27 and 230. The materials were subsequently calcined to generate the gold nanoparticles. No reduction step was described in the work; consistent with that numerous methods including XPS and XAS indicated the gold was in a variety of oxidation states. Glomm et al. [35] reported the synthesis of Au-OMS nanocomposites using (i) in situ growth of nanoparticles during OMS synthesis, (ii) template loading where

preformed 5 and 10 nm Au colloids were added to the OMS synthesis, and (iii) diffusion loading where preformed 5 and 10 nm Au colloids were added to the OMS after synthesis. They concluded that in all three cases the majority of the Au particles were on the OMS exterior surface, but with the fraction residing internally being higher in cases (i) and (ii). King et al. [36] used a liquid crystal templating approach to form metal nanoparticle (including Au) OMS composites. In their work a true H1 phase was formed using the surfactant $C_{12}EO_8$, metal salts and water. XPS indicated the gold particles formed were Au^0 and TEM indicated many of the particles were formed in the OMS pores. This work was extended, as described below, to bimetallic systems.

2.1.3. Impregnation with preformed nanocrystals

In addition to the work by Glomm et al. [35] other groups have reported Au-OMS composites using preformed Au nanocrystals. Gupta et al. [37] have reported the uptake of Au nanocrystals 2 nm in diameter into SBA-15 materials. Using TEM and nitrogen porosimetry the authors showed that the majority of the nanocrystals were inside the mesopores, in contrast with the findings of Glomm et al. [35]. This was ascribed to the use of supercritical CO_2 as the media for nanoparticle impregnation. Also of note this paper nicely summarizes some of the previous work in the area of impregnating OMS phases with preformed nanocrystals.

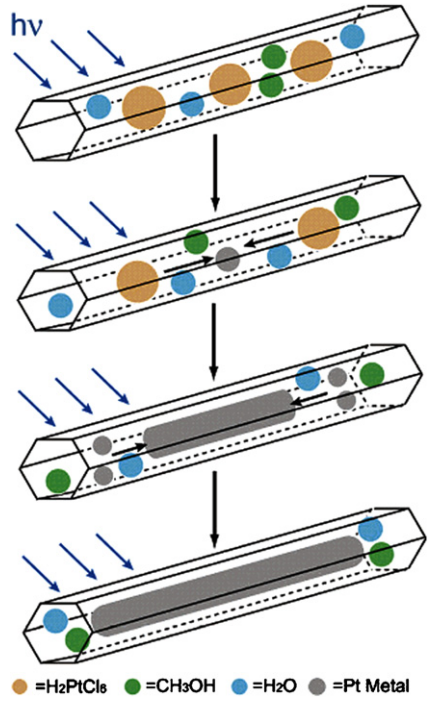

Fig. 6. Proposed mechanism for the formation of Pt wires in HMM-1. Figure used from Ref. [41] with permission of the American Chemical Society.

2.2. Platinum

2.2.1. Post-synthetic deposition and other reagent impregnation methods

Several labs have also investigated the synthesis of platinum nanocrystals in OMS materials. Chao et al. [38], for instance, used a functionalized MCM-41 material similar to Ref. [25] to form platinum nanoparticles and networks after reduction. Additional work from Chao's lab [39] has extended this approach to cubic MCM-48 materials. The authors showed TEM images indicating that nanoparticles, rods, tripods, and wire networks can be formed in the MCM-48 pores. The authors claimed that changes in the morphology of the metal were due to differing solvent contents during impregnation, though the details in the paper were fairly sparse. Chytil et al. [40] have used deposition–precipitation methods to prepare platinum nanoparticles in SBA-15. The materials formed were compared to those made using typical wet impregnation methods. The authors found that the deposition–precipitation method on whole led to smaller particles and a higher fraction of the particles forming in the SBA-15 pores. Sakamoto et al. [41] have reported the formation of nanoparticles and nanowires in HMM-1. The unique feature of this work was that the authors showed that using the same wet impregnation method very different nanostructures could be formed using different reduction methods. The authors showed that nanowires formed when UV light (100 W, 250–600 nm) was used for the reduction and nanoparticles were formed when typical reduction procedures (H_2 gas, 673 K) are used. Fig. 6 shows a mechanism proposed by the authors for the photochemical reduction. In a subsequent paper [42] the same researchers extended this to FSM-16.

2.2.2. Direct synthesis methods

The reports of Pt-OMS materials via direct synthesis methods are sparse. The paper by King et al. [36] above describing direct synthesis of gold nanoparticles also discusses Pt-OMS materials as well. Krawiec et al. [43] have reported the fabrication of MCM-41/Pt composites by adding the platinum precursor to the synthesis mixture (Fig. 7). The particles are formed in situ during the surfactant calcination. Using a variety of methods the authors show the particles selectively form in the MCM-41 pores.

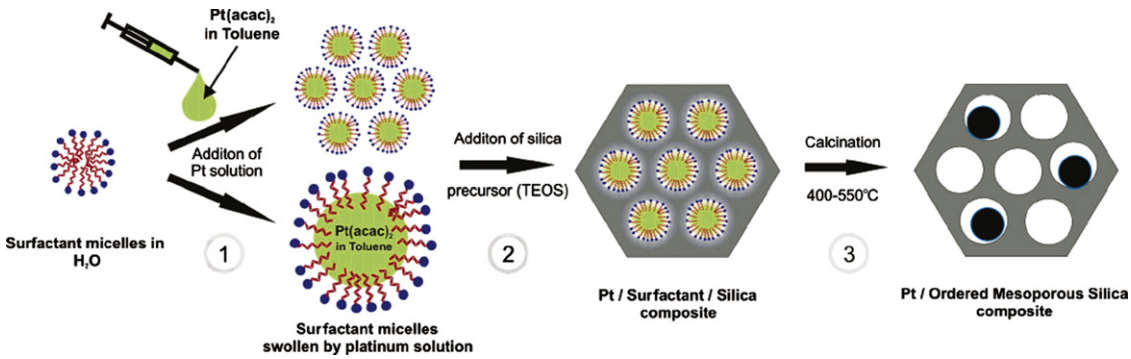

Fig. 7. Synthesis scheme for the preparation of Pt/MCM-41 composites employed by Krawiec and coworkers. Figure used from Ref. [43] with permission of the American Chemical Society.

The authors also show that this concept works for a variety of other metals and metal oxides.

2.2.3. Impregnation with preformed nanoparticles

In contrast to work described above for gold, there are several reports of forming composites via addition of preformed nanoparticles. Chytil et al. [44] have reported work forming Pt nanoparticles via reduction of platinum salts in the presence of the triblock copolymer used to make SBA-15 (Pluronic P123). These particle–polymer complexes were then used in the SBA-15 synthesis. Using multiple characterization methods the authors reported that a fraction of the particles are occluded in the SBA-15 mesopores.

Collaborative work between Somorjai's and Yang's labs at UC Berkeley has led to a series of papers reporting on the synthesis of platinum nanoparticles in OMS materials. In one report [45] platinum nanoparticles between 1.7 and 7.1 nm in size were made by alcohol reduction and stabilized with PVP. These particles were incorporated into the SBA-15 support using low-power sonication. Numerous methods were used to characterize the particles, including catalytic testing. Konya et al. [46] have reported a follow-up to this study. In another report by Song et al. [47] platinum nanoparticles were mixed with Pluronic P123 (SBA-15 template), TMOS, and NaF, as the synthesis pH was near neutral as compared to typical SBA-15 syntheses which employ acidic conditions. The results indicated a high fraction of particles were occluded in the pores of SBA-15. In a follow-up paper to this work, Rioux et al. [48] reported an extension of the work by Song and coworkers using platinum nanocrystals of different morphologies to study this effect on reactivity.

2.3. Palladium

2.3.1. Post-synthetic deposition and other reagent impregnation methods

Many of the works reported on palladium/OMS composites have been motivated by catalyst design for the Heck and Suzuki reactions and partial or selective liquid phase hydrogenations of alkenes and alkynes. In general terms many of the same conceptual themes observed above for gold and platinum are found to hold for palladium as well. Behrens and Spittel [49] reported the synthesis of Pd-MCM-41 composites using a $Pd_8(CO)_8(PMe_3)_7$ cluster which, upon mild thermal treatment, decomposes to yield Pd nanoparticles. The authors compared this composite to Pd-MCM-41 samples made using other methods and showed that the carbonyl precursor led to the smallest particles. Das and Sayari [50] reported the synthesis of pore-expanded MCM-41 and its use for forming Pd nanoparticles using borohydride reduction. Using TEM/STEM the authors claimed the majority of the particles were located in the OMS pores. Li et al. [51] reported that SBA-15 grafted with trimethoxysilane could be subsequently treated with palladium acetate in THF to yield palladium nanoparticles in SBA-15. There is little characterization of the resulting composite material beyond XPS and catalytic testing. Jiang and Gao [52] have reported Pd nanoparticles formed in SBA-15/PAMAM dendimer composites using the PAMAM dendrimer as a template. Marin-Astorga et al. [53] reported Pd/OMS materials using a variety of OMS substrates (HMS, MSU-X, and MCM-41). TEM and H_2 chemisorption indicated most of the particles, formed by impregnation of $Pd(acac)_2$ in toluene followed by drying and reduction in hydrogen, were below 4 nm in size. The work by Fukuoka et al. [54] described above has also been extended to palladium systems.

There have also been reports in the case of palladium of selectively forming nanoparticles in the micropores of SBA-15.

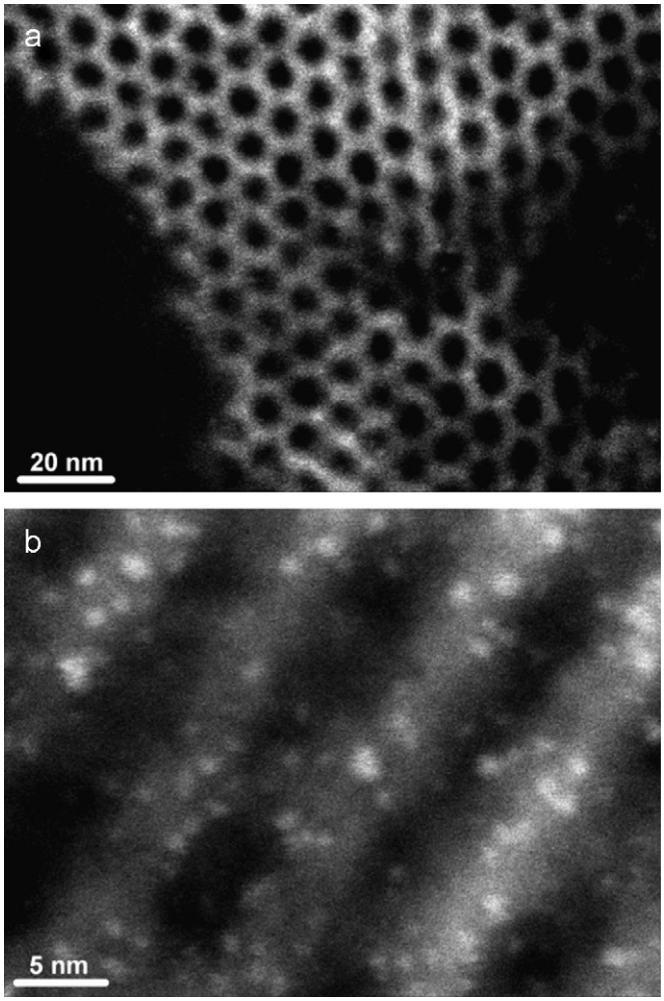

Fig. 8. STEM images of Pd/SBA-15 sample viewed along (a) and perpendicular to (b) the axis of the hexagonally arranged mesopores. Figure used from Ref. [56] with permission of the American Chemical Society.

One report by Yuranov et al. [55] using conventional impregnation methods claimed to selectively form Pd nanoparticles in the micropores of SBA-15 (located in the pore walls). However the evidence for this was minimal. Recent work by Yang et al. [56] presented much stronger evidence for selective incorporation of Pd nanoparticles into the micropores of SBA-15. Numerous methods, most notably STEM images (Fig. 8) were used to make a strong case that the Pd particles do not occupy the mesopores of SBA-15.

2.3.2. Direct synthesis methods

Han et al. [57] reported the synthesis of Pd/SBA-15 by inclusion of palladium salts in the synthesis mixture under a reducing environment. This work is similar to the work done by Krawiec et al. [43] above. Based on XRD (Scherrer equation) and TEM results the authors claimed the particles were in the SBA-15 pores. Mastalir et al. [58] report the formation of Pd/MCM-41 using two different direct synthesis methods. In one approach the nanoparticles were formed by mixing surfactant with the palladium salt, and after aging was added to the MCM-41 synthesis mixture. The other approach was to not age the surfactant palladium salt mixture prior to silicate addition. The authors reported that the former method led to Pd particles primarily on the outer surface of the MCM-41 particles, whereas the latter led to Pd particles occluded in the MCM-41 pores.

2.3.3. Impregnation with preformed nanoparticles

Demel et al. [59,60] have reported two works where preformed palladium nanoparticles (thermochemical reduction of palladium (II) acetate in propylene carbonate or in THF) were impregnated into MCM-41. Nitrogen adsorption indicates a significant reduction in pore volume after particle impregnation. However, TEM images were inconclusive about the location of the particles and no particle size distributions were given.

2.4. Other metals

2.4.1. Iron

Two papers [61,62] have reported the synthesis and characterization of iron nanowires via impregnation of iron pentacarbonyl followed by decomposition using UV irradiation in vacuum and subsequent reduction in hydrogen. TEM and electron diffraction were used to estimate the nanowire size and crystallinity. SQUID was used to measure the magnetic properties of the samples. It was observed that higher reduction temperatures led to smaller nanowires that possessed higher coercive forces values (up to 80 Oe at room temperature).

2.4.2. Bismuth

The Holmes' lab in Ireland has reported the synthesis of bismuth nanoparticles/nanowires in SBA-15-type materials [63]. The authors used triphenylbismuth in supercritical or near supercritical toluene to load the bismuth precursor into the OMS powder. The mixture was then heated to between 523 and 673 K to decompose the triphenyl bismuth compound into nanoclusters. The work reported numerous methods to demonstrate formation of bismuth nanowires, and it was observed that the highest loadings of bismuth were achievable when the reaction conditions were near the critical point of toluene.

2.4.3. Germanium

The Holmes' lab has also reported the synthesis of germanium nanowires in OMS thin films and anodized aluminum oxide (AAO) membranes. Similar to the work described above the authors used decomposition of an organogermanate compound (diphenylgermante) in supercritical CO_2. The nanocomposites were thoroughly characterized using methods including conductive AFM to probe the electrical properties of the nanowires formed. In contrast to the work reported for bismuth, no description was given about controlling wire formation by changing decomposition conditions, however, the conductive AFM results showed the germanium nanowires were conducting and indicated a high degree of uniformity in terms of individual nanowire behavior. A recent paper from the same lab [64] demonstrated that using the same synthesis approach for powder OMS samples one can change the germanium nanowire diameter by changing the pore size of the OMS matrix. Numerous characterization methods including adsorption, EM, and X-ray spectroscopy supported this conclusion as well as the fact that elevated melting temperatures as compared to bulk germanium were observed.

2.4.4. Cobalt

Rice et al. [65] have also used the same OMS film/CO_2 supercritical fluid inclusion method described above to make cobalt nanowires. Besides using cobalt as the inclusion method the work reported also utilized lithographically patterned surfaces upon which to grow OMS films wherein the pores are aligned parallel to the etched channels (Fig. 9). The authors reported these films had slightly different properties as compared to films previously reported by these labs. Again, numerous characterization methods including diffraction, scattering, and microscopy were used to characterize the films and the wires in the OMS pores. In the work reported cobalt carbonyl was used as the metal precursor.

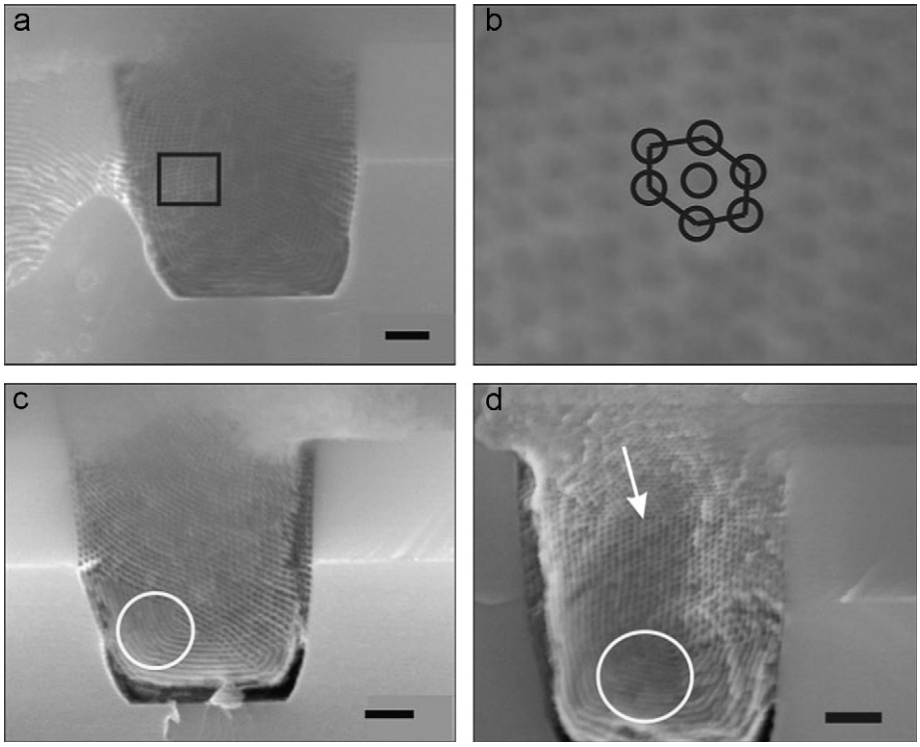

Fig. 9. HR-SEM images showing the channels with Co filled hexagonal arrangements of pores. (b) The boxed area in (a). The areas circled in (c) and (d) show pore arrangements that are nor parallel to the pore wall and originate in corners. The arrow shows an area similar to a grain boundary. The scale bar represents 100 nm in all figures. Figure used from Ref. [65] with permission from Wiley VCH.

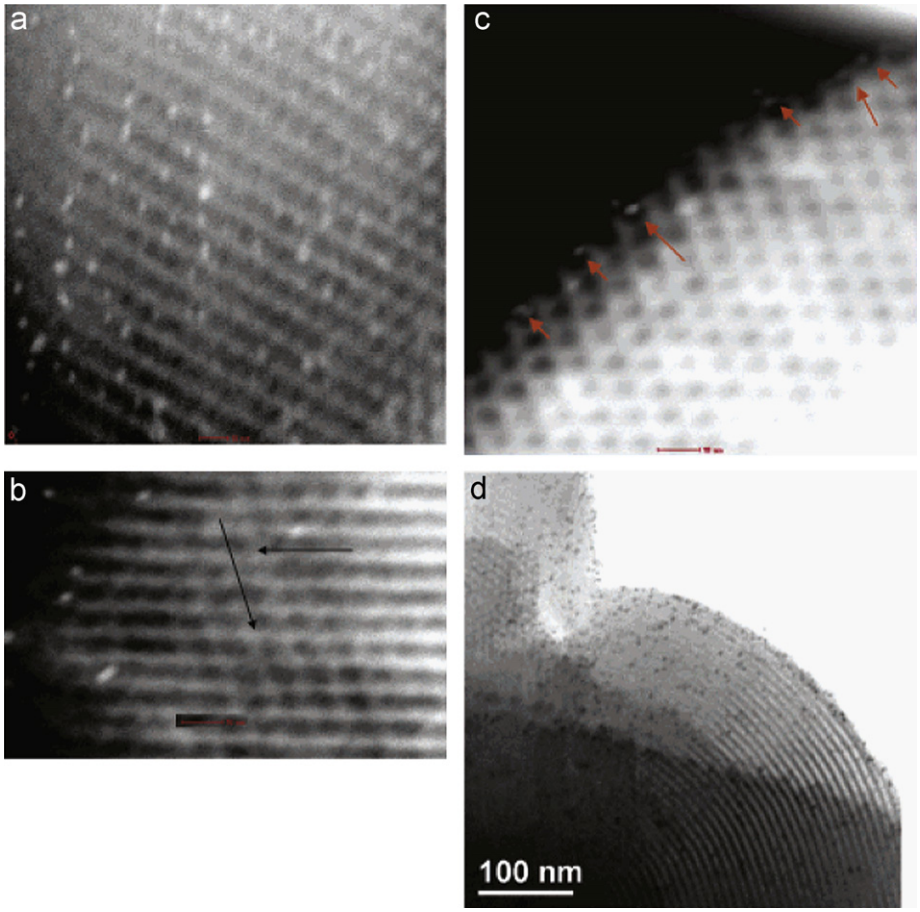

Fig. 10. (a) *Z* contrast STEM (planar view) of MPS infused with Ir-TOAB, (b) out of focus view of (a), (c) top down view of (a), and (d) TEM micrograph of MPS infused with Ir-TOAB nanocrystals without any pretreatment. Scale bars (a–c) are 10 nm. Figure used from Ref. [67] used with permission from the American Chemical Society.

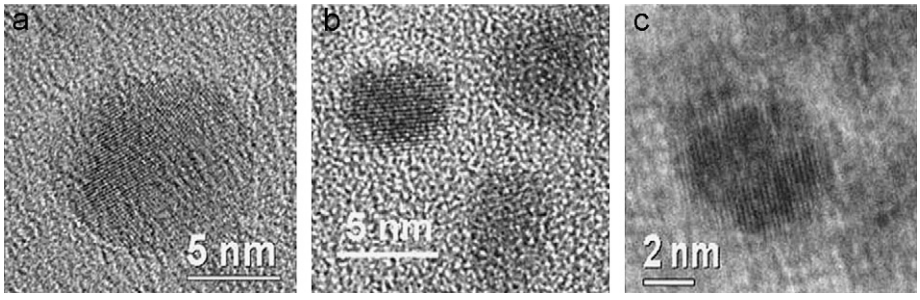

Fig. 11. HRTEM images of bimetallic nanoparticles encapsulated in mesoporous silicates: (a) PdAu, (b) PtCo, and (c) PdRu. Figure used from Ref. [70] used with permission from the Royal Society of Chemistry.

2.4.5. Other systems

Some of the works reported do not fit nicely into any of the categories above. For instance, a recent publication of collaborative work between the Holmes and Bein labs [66] demonstrated the formation of a variety of metallic (Au, Pt, Pd) and conducting (Ge) nanowires formed in OMS phases synthesized in AAO membranes. The unique feature of this work was not the methods employed to generate the metal nanostructures, but rather the integration of the composite (AAO-OMS) ceramic membrane as a substrate. Gupta et al. [67] have reported the formation of iridium-SBA-15 composites by impregnating preformed Ir nanocrystals into SBA-15 using toluene/supercritical CO_2. Both the precursor materials (Ir nanocrystals and SBA-15) as well as the nanocomposite are thoroughly characterized and those results, including *Z* contrast STEM shown in Fig. 10, indicate the nanocrystals are primarily in the mesopores.

3. Bimetallics

By contrast to the reports of single metal nanoparticles, there is a relative dearth of literature in the area of bimetallic compounds. Beyond the early work from Thomas' lab [17,68,69] reporting bimetallic particles formed via decomposition of mixed metal carbonyl precursors, the literature in this area is sparse. Based on some of the reports below the authors believe this area is rich for future studies.

King et al. [70] reported the synthesis of several bimetallic nanoparticle systems in OMS using the liquid crystal templating described above. The authors emphasized in particular the formation of PtCo, PdAu, and PdRu as for these systems elemental composition (by EDX), TEM, adsorption and diffraction data were reported (Fig. 11). Also the magnetic properties of the PtCo system were reported. While it appears the nanoparticles formed are not

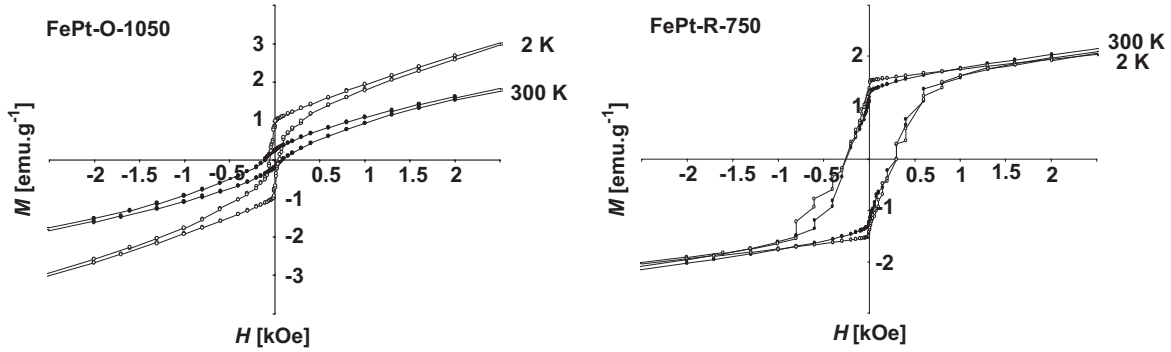

Fig. 12. Isothermal magnetization versus field hysteresis loops measured at 2 and 300 K for FePT OMS nanocomposites (left) formed under oxidizing conditions and reduced at 1050 °C and (right) formed under reducing conditions and reduced at 750 °C. Figure used from Ref. [71] with permission from Wiley-VCH.

of the quality observed in many solution phase syntheses, the approach clearly has promise. Kockrick et al. [71] reported the synthesis of FePt particles made by simple incipient wetness impregnation of iron and platinum salts followed by reduction. The resulting materials were characterized using diffraction, microscopy, and Mössbauer spectroscopy and shown to be fct-FePt nanocrystals. The authors claimed the OMS matrix stabilizes the nanocrystals formed. Magnetic data for these materials is shown in Fig. 12. In work conceptually similar to that by Thomas' lab, Schweyer-Tihay et al. [72] used $NEt_4[Co_3Ru(CO)_{12}]$ clusters to form nanoparticles in MCM-41. The authors observed that thermal treatments below 270 °C result in pure Ru and Co nanoparticles (i.e. no bimetallics). At higher temperatures alloying was observed with increasing temperatures leading to increasing Ru content in the nanoparticles, ultimately reaching a 3:1 Co:Ru stoichiometry. The magnetic measurements performed, along with XRD facilitated observation of this behavior.

4. Non-metals

In addition to work on metal nanoparticles, there are numerous reports of metal chalcogenides, most notably ZnS, CdS, and ZnSe. The investigation of these materials, while extremely interesting, has been sufficiently reviewed elsewhere [73–75]. There are also numerous reports of metal oxide clusters OMS phases which have similarly been reviewed previously. However, one area that has been only sparingly investigated is the synthesis of supported metal carbide/nitride/phosphide clusters on OMS. A recent report by Hu et al. [76] reports on the formation of tungsten carbide clusters in SBA-15 formed via reduction of tungsten oxide precursors. Finally, while outside the time range surveyed here, it is noteworthy that there is a report of Co_2P nanoparticles formed in OMS materials via grafting of a phosphine complex followed by decomposition [77]. The lack of literature in this area will be discussed in more detail below.

5. Future prospects, challenges, and opportunities

As one can see the catalysis community has been the driving force behind work in this area. The consequence is that the bulk of the effort has been on using powders as a support, a focus on late transition metal particles, and the reliance of catalytic testing to evaluate metal properties, at times at the expense of other analytical methods. Homogeneity of the supported metal phase will prove crucial as the field moves to areas such as optical/magnetic materials.

Advances in the ability to synthesize high-quality thin films of OMS phases will also usher in new possibilities. For example, recent works from the Hillhouse lab at Purdue demonstrate that the ability to fabricate OMS films with interconnected pores reproducibly offers new opportunities [78,79]. The development of robust synthesis methods for OMS thin films holds great opportunities for advances in the construction of more complex materials that will be relevant in fields potentially including optics, ion-conductors, and magnetic materials. In this context the works from Holmes' lab reviewed above are particularly noteworthy and moving towards this end.

5.1. Challenges and opportunities

Homogeneity of the occluded nanoparticles/wires is still a considerable challenge. The work reviewed above indicates that supercritical fluid-based impregnation methods, both of reagents and preformed particles, seem to lead to the most homogeneous materials. Expanding this to loadings where true pore filling is achieved to fabricate wires will likely prove challenging. It seems probable that many of the "simple" impregnation schemes will lead to non-selective metal deposition on the outer surface of the OMS phase at high loadings. One possibility would be to use a combined scheme of direct synthesis methods to deposit an initial metal particulate phase in the mesopores, followed by a supercritical impregnation step to achieve high loadings.

The main opportunities in this area would appear to be twofold. First, the relative dearth of nanostructured phases beyond simple late transition metals and metal chalcogenides (e.g. ZnS, ZnSe) indicates that there is still a rich amount of chemistry that has been unexplored. The relatively few papers on bimetallic or binary nanoparticles are consistent with this point. The future will likely see a dramatic increase in this area given that the catalytic properties of bimetallic particles are of significant interest. The unique magnetic properties of, for instance the FePt phases, will also spur growth in this area. It should also be pointed out that while these materials will likely display interesting properties, their characterization will prove non-trivial. Second, there is still considerable scope for developing devices based on OMS film—nanowire composites. While this second opportunity is a longer-term problem than the first one, at a minimum it should lead to a wealth of basic scientific information about how metal/metal chalcogenide and other nanostructured phases behave in a solid matrix.

Acknowledgment

The authors acknowledge the National Science Foundation (CTS-0329386, CTS-0624813) for supporting their research in OMS materials.

References

[1] S. Beck, J.C. Vartuli, W.J. Roth, M.E. Leonowicz, C.T. Kresge, K.D. Schmitt, C.T.W. Chu, D.H. Olson, E.W. Sheppard, S.B. McCullen, J.B. Higgins, J.L. Schlenker, J. Am. Chem. Soc. 114 (1992) 10834–10843.
[2] C.T. Kresge, M.E. Leonowicz, W.J. Roth, J.C. Vartuli, J.S. Beck, Nature 359 (1992) 710–712.
[3] U. Ciesla, F. Schüth, Micropor. Mesopor. Mater. 27 (1999) 131–149.
[4] M.E. Davis, Nature 417 (2002) 813–821.
[5] K. Moller, T. Bein, Chem. Mater. 10 (1998) 2950–2963.
[6] F. Schüth, W. Schmidt, Adv. Mater. 14 (2002) 629–638.
[7] A. Stein, Adv. Mater. 15 (2003) 763–775.
[8] A. Stein, B.J. Melde, R.C. Schroden, Adv. Mater. 12 (2000) 1403–1419.
[9] A. Corma, Chem. Rev. 97 (1997) 2373–2419.
[10] A. Corma, H. Garcia, Chem. Rev. 103 (2003) 4307–4365.
[11] C. Li, Catal. Rev. 46 (2004) 419–492.
[12] A. Taguchi, F. Schuth, Micropor. Mesopor. Mater. 77 (2005) 1–45.
[13] D.M. Ford, E.E. Simanek, D.F. Shantz, Nanotechnology 16 (2005) S458–S475.
[14] D. Astruc, F. Lu, J.R. Aranzaes, Angew. Chem. Int. Ed. 44 (2005) 7852–7872.
[15] L.M. Bronstein, Top. Curr. Chem. 226 (2003) 55–89.
[16] J.D. Holmes, D.M. Lyons, K.J. Ziegler, Chem. Eur. J. 9 (2003) 2144–2150.
[17] B.F.G. Johnson, Top. Catal. 24 (2003) 147–159.
[18] S. Günter, Clusters and Colloids: From Theory to Applications, VCH, Weinheim, 1994.
[19] M. Haruta, N. Yamada, T. Kobayashi, S. Iijima, J. Catal. 115 (1989) 301–309.
[20] M. Haruta, S. Tsubota, T. Kobayashi, H. Kageyama, M.J. Genet, B. Delmon, J. Catal. 144 (1993) 175–192.
[21] J.P. Gabaldon, M. Bore, A.K. Datye, Top. Catal. 44 (2007) 253–262.
[22] M.T. Bore, H.N. Pham, T.L. Ward, A.K. Datye, Chem. Commun. (2004) 2620–2621.
[23] M.T. Bore, H.N. Pham, E.E. Switzer, T.L. Ward, A. Fukuoka, A.K. Datye, J. Phys. Chem. B 109 (2005) 2873–2880.
[24] M.T. Bore, M.P. Mokhonoana, T.L. Ward, N.J. Coville, A.K. Datye, Micropor. Mesopor. Mater. 95 (2006) 118–125.
[25] K.-J. Chao, M.-H. Cheng, Y.-F. Ho, P.-H. Liu, Catal. Today 97 (2004) 49–53.
[26] P.-H. Liu, Y.-P. Chang, T.-H. Phan, K.-J. Chao, Mater. Sci. Eng. C 26 (2006) 1017–1102.
[27] T. Nakamura, Y. Yamada, K. Yano, J. Mater. Chem. 17 (2007) 3726–3732.
[28] K. Yano, Y. Fukushima, J. Mater. Chem. 14 (2004) 1579–1584.
[29] M. Bandyophadhyay, O. Korsak, M.W.E. van den Berg, W. Grunert, A. Birkner, W. Li, F. Schuth, H. Gies, Micropor. Mesopor. Mater. 89 (2006) 158–163.
[30] W. Yan, B. Chen, S.M. Mahurin, E.W. Hagaman, S. Dai, S.H. Overbury, J. Phys. Chem. B 108 (2004) 2793–2796.
[31] C. Kan, W. Cai, C. Li, G. Fu, L. Zhang, J. Appl. Phys. 96 (2004) 5727–5734.
[32] C.-K. Tsung, W. Hong, Q. Shi, X. Kou, M.H. Yeung, J. Wang, G.D. Stucky, Adv. Func. Mater. 16 (2006) 2225–2230.
[33] M. Chatterjee, Y. Ikushima, Y. Hakuta, H. Kawanami, Adv. Synth. Catal. 348 (2006) 1580–1590.
[34] D.B. Akolekar, S.K. Bhargava, J. Mol. Catal. A: Chem. 236 (2005) 77–86.
[35] W.R. Glomm, G. Oye, J. Walmsley, J. Sjoblom, J. Disp. Sci. Technol. 26 (2005) 729–744.
[36] N.C. King, R.A. Blackley, W. Zhou, D.W. Bruce, Chem. Commun. (2006) 3411–3413.
[37] G. Gupta, P.S. Shah, X. Zhang, A.E. Saunders, B.A. Korgel, K.P. Johnston, Chem. Mater. 17 (2005) 6728–6738.
[38] K.-J. Chao, Y.-P. Chang, Y.-C. Chen, A.S. Lo, T.-H. Phan, J. Phys. Chem. B 110 (2006) 1638–1646.
[39] X.-J. Guo, C.-M. Yang, P.-H. Liu, M.-H. Cheng, K.-J. Chao, Cryst. Growth Des. 5 (2005) 33–36.
[40] S. Chytil, W.R. Glomm, I. Kvande, T. Zhao, J.C. Walmsley, E.A. Blekkan, Top. Catal. 45 (2007) 93–99.
[41] Y. Sakamoto, A. Fukuoka, T. Higuchi, N. Shimomura, S. Inagaki, M. Ichikawa, J. Phys. Chem. B 108 (2004) 853–858.
[42] A. Fukuoka, M. Ichikawa, Top. Catal. 40 (2006) 103–109.
[43] P. Krawiec, E. Kockrick, P. Simon, G. Auffermann, S. Kaskel, Chem. Mater. 18 (2006) 2663–2669.
[44] S. Chytil, W.R. Glomm, E. Vollebekk, H. Bergem, J. Walmsley, J. Sjoblom, E.A. Blekkan, Micropor. Mesopor. Mater. 86 (2005) 19–206.
[45] R.M. Rioux, H. Song, J.D. Hoefelmeyer, P. Yang, G.A. Somorjai, J. Phys. Chem. B 109 (2005) 2192–2202.
[46] Z. Konya, E. Molnar, G. Tasi, K. Niesz, G.A. Somorjai, I. Kiricsi, Catal. Lett. 113 (2007) 19–28.
[47] H. Song, R.M. Rioux, J.D. Hoefelmeyer, R. Kormor, K. Niesz, M.G. Grass, P. Yang, G.A. Somorjai, J. Am. Chem. Soc. 128 (2006) 3027–3037.
[48] R.M. Rioux, H. Song, M. Grass, S. Habas, K. Niesz, J.D. Hoefelmeyer, P. Yang, G.A. Somorjai, Top. Catal. 39 (2006) 167–174.
[49] S. Behrens, G. Spittel, Dalton Trans. (2005) 868–873.
[50] D.D. Das, A. Sayari, J. Catal. 246 (2007) 60–65.
[51] L. Li, J.-L. Shi, J.-N. Yan, Chem. Commun. (2004) 1990–1991.
[52] Y. Jiang, Q. Gao, J. Am. Chem. Soc. 128 (2006) 716–717.
[53] N. Marin-Astorga, G. Pecchi, T.J. Pinnavaia, G. Alvez-Manoli, P. Reyes, J. Mol. Catal. A: Chem. 247 (2006) 145–152.
[54] A. Fukuoka, H. Araki, J.-I. Kimura, Y. Sakamoto, T. Higuchi, N. Sugimoto, S. Inagaki, M. Ichikawa, J. Mater. Chem. 14 (2004) 752–756.
[55] I. Yuranov, L. Kiwi-Minsker, P. Buffat, A. Renken, Chem. Mater. 16 (2004) 760–761.
[56] C.-M. Yang, H.-A. Lin, B. Zibrowius, B. Spliethoff, F. Schuth, S.-C. Liou, M.-W. Chu, C.-H. Chen, Chem. Mater. 19 (2007) 3205–3211.
[57] P. Han, X. Wang, X. Qiu, X. Ji, L. Gao, J. Mol. Catal. A: Chem. 272 (2007) 136–141.
[58] A. Mastalir, B. Rac, Z. Kiraly, A. Molnar, J. Mol. Catal. A: Chem. 264 (2007) 170–178.
[59] J. Demel, J. Cejka, S. Bakardjieve, P. Stepnicka, J. Mol. Catal. A: Chem. 263 (2007) 259–263.
[60] J. Demel, J. Cejka, P. Stepnicka, J. Mol. Catal. A: Chem. 274 (2007) 127–132.
[61] A.A. Eliseev, K.S. Napolskii, A.V. Lukashin, Y.D. Tretyakov, J. Magn. Magn. Mater. 272–276 (2004) 1609–1611.
[62] N.A. Grigorieva, S.V. Grigoriev, A.I. Okorokov, H. Eckerlebe, A.A. Eliseev, K.S. Napolskii, Physica E 28 (2005) 286–295.
[63] J. Xu, W. Zhang, M.A. Morris, J.D. Holmes, Mater. Chem. Phys. 104 (2007) 50–55.
[64] G. Audoit, J.S. Kulkarni, M.A. Morris, J.D. Holmes, J. Mater. Chem. 17 (2007) 1608–1613.
[65] R.K. Rice, D.C. Arnold, M.T. Shaw, D. Iacopina, A.J. Quinn, H. Amenitsch, J.D. Holmes, M.A. Morris, Adv. Func. Mater. 17 (2007) 133–141.
[66] N. Petkov, B. Platschek, M.A. Morris, J.D. Holmes, T. Bein, Chem. Mater. 19 (2007) 1376–1381.
[67] G. Gupta, C.A. Stowell, M.N. Patel, X. Gao, M.J. Yacaman, B.A. Korgel, K.P. Johnston, Chem. Mater. 18 (2006) 6239–6249.
[68] J.M. Thomas, R. Raja, B.F.G. Johnson, S. Hermans, M.D. Jones, T. Khimyak, Ind. Eng. Chem. Res. 42 (2003) 1563–1570.
[69] D. Ozkaya, W. Zhou, J.M. Thomas, P. Midgley, V.J. Keast, S. Hermans, Catal. Lett. 60 (1999) 113–120.
[70] N.C. King, R.A. Blackley, M.L. Wears, D.M. Newman, W. Zhou, D.W. Bruce, Chem. Commun. (2006) 3414–3416.
[71] E. Kockrick, P. Krawiec, W. Schnelle, D. Geiger, M. Schappacher, R. Pottgen, S. Kaskel, Adv. Mater. 19 (2007) 3021–3026.
[72] F. Schweyer-Tihay, C. Estournes, P. Braunstein, J. Guille, J.-L. Paillaud, M. Richard-Plouet, J. Rose, Phys. Chem. Chem. Phys. 8 (2006) 4018–4028.
[73] L. Chen, P.J. Klar, W. Heimbrodt, T. Kurz, H.A.K. von Nidda, A. Loidl, A.V. Kouzema, M. Froba, Phys. Status Solidi (b) 243 (2006) 831–834.
[74] A.V. Kouzema, M. Froba, L. Chen, P.J. Klar, W. Heimbrodt, Adv. Func. Mater. 15 (2005) 168–172.
[75] F.J. Brieler, P. Grundmann, M. Froba, L.M. Chen, P.J. Klar, W. Heimbrodt, H.A.K. von Nidda, A. Loidl, Eur. J. Inorg. Chem. 18 (2005) 3597–3611.
[76] L. Hu, S. Ji, Z. Jiang, H. Song, P. WU, Q. Liu, J. Phys. Chem. C 111 (2007) 15173–15184.
[77] F. Schweyer-Tihay, P. Braunstein, C. Estournes, J.L. Guille, B. Lebeau, J.-L. Paillaud, M. Richard-Plouet, J. Rose, Chem. Mater. 15 (2003) 57–62.
[78] T.C. Wei, H.W. Hillhouse, Langmuir 23 (2007) 5689–5699.
[79] V.N. Urade, T.C. Wei, M.P. Tate, J.D. Kowalski, H.W. Hillhouse, Chem. Mater. 19 (2007) 768–777.